

Peak mobilities in low-symmetry silicon inversion layers

H. Closs, J. B. Veiga Salles, and J. R. Senna

*Laboratório Associado de Sensores e Materiais, Instituto de Pesquisas Espaciais, Caixa Postal 515,
12201 São José dos Campos, São Paulo, Brazil*

(Received 14 November 1988)

We have measured the magnitude and corresponding surface carrier density of the 4.2-K peak mobilities of silicon inversion layers tilted 0° to 43° from the (001) plane by a rotation around the $[1\bar{1}0]$ direction. Comparison between experiments and our calculations of mobility for anisotropic inversion layers gives strong evidence for anisotropy of scattering potentials.

The peak mobility of inversion-layer electrons at low (4.2 K) temperatures is commonly used to characterize the quality of a silicon metal-oxide-semiconductor field-effect transistor (MOSFET) sample, as its magnitude μ_p and corresponding surface carrier concentration n_p depend on the amount of competitive scattering by ionic charges in the oxide near the Si-SiO₂ interface, which decreases with electron Fermi wave vector, and scattering by roughness in that interface, which increases with k_F . A universal behavior was observed by Cham and Stern¹ to hold for these quantities in Si(001) inversion layers: they have shown that available experimental data obeyed an empirical relation of the form

$$\mu_p = \mu_0 [n_p / (10^{12} \text{ cm}^{-2})]^{-\alpha} \quad (1)$$

with $\alpha = 1.6$ and $\mu_0 = 1.2 \times 10^4 \text{ cm}^2 \text{ V}^{-1} \text{ s}^{-1}$.

Such a behavior is represented in Fig. 1 by a dotted-dashed straight line in the log-log plot of μ versus n_s ; the dispersion in the experimental data collected by Cham and Stern would be equivalent to $(\Delta \log_{10} \mu_0 / \log_{10} \mu_0) \approx \pm 5\%$.

In this Brief Report, we show that this behavior is quantitatively explained by simple linear-scattering theory, and then analyze experimental data we have obtained for the $\mu_p(n_p)$ dependence of inversion layers with orientation different from (001). By comparing these results with a calculation that takes into account the intrinsic Fermi-surface anisotropy in these samples, we show that the data are not explained by this intrinsic anisotropy alone, but rather reflect a systematic dependence of the material parameters (surface roughness and impurity concentration) on the interface orientation.

Calculations by Gold,² including multiple-scattering effects, have given good agreement with the experimental $\mu(n_s)$ dependence in the full range of density, and provided an excellent fit to the experimental data on the $\mu_p(n_p)$ dependence in (001) samples (dashed straight line in Fig. 1). The inclusion of multiple-scattering effects is crucial for obtaining the correct shape of the $\mu(n_s)$ curve, especially at low n_s , where the localization effects are most evident. For the densities n_p corresponding to the peak mobilities, however, linear-scattering theory is sufficient to account for the relation expressed by Eq. (1). In Fig. 1 we show the results of a calculation of $\mu(n_s)$ by the simple linear-scattering theory, as described by Matsumoto and Uemura,³ and by Ando.⁴ In this approximation the

inverse mobilities limited by charged impurities in the oxide (characterized by a surface density N_{ox}) and by the Si-SiO₂ interface roughness (characterized by a rms fluctuation Δ with correlation length Λ) are additive, and the figure illustrates the effect of the change of parameters N_{ox} , Δ , and Λ .

The solid straight line shows the dependence of μ_p on n_p , for the same parameters $N_d = 3.6 \times 10^{11} \text{ cm}^{-2}$ and $\Lambda = 15 \text{ \AA}$ as in Ref. 2, but with $\Delta = 4.3 \text{ \AA}$, a value closer to the ones which come out from full N_s range fittings of

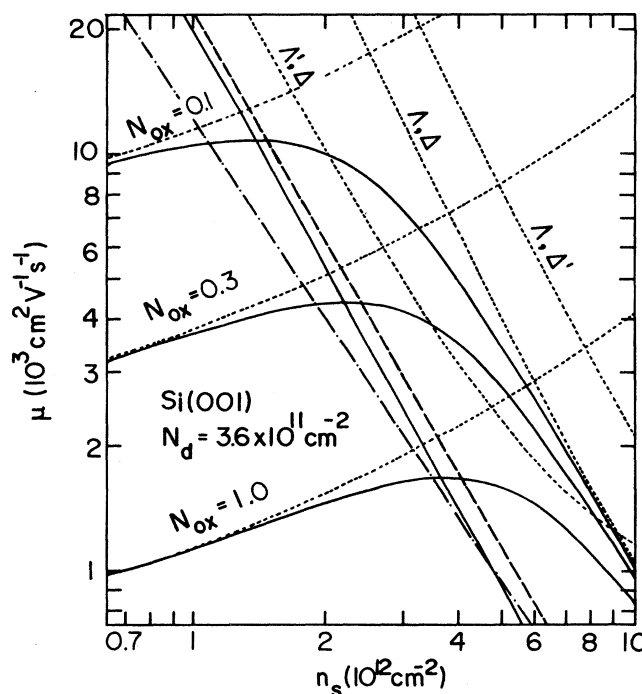


FIG. 1. Dotted curves: Si(001) mobilities limited by charged impurities located in the Si-SiO₂ interface, for several values of N_{ox} (expressed in units of 10^{12} cm^{-2}) and limited by surface roughness, for several values of rms fluctuation Δ of the interface, with correlation length Λ ($\Lambda = 15 \text{ \AA} = 30 \text{ \AA}$, $\Delta = 4.3 \text{ \AA}$, $\Delta' = 3.0 \text{ \AA}$). Solid curves: resulting mobilities at zero temperature, for $\Lambda = 15 \text{ \AA}$ and $\Delta = 4.3 \text{ \AA}$. Solid straight line: corresponding $\mu_p(n_p)$ relation. Dotted-dashed line: $\mu_p(n_p)$ reported by Cham and Stern (Ref. 1). Dashed line: $\mu_p(n_p)$ calculated by Gold (Ref. 2).

mobility by linear-scattering theory.³ N_d is the depletion-layer surface charge density. The solid straight line in Fig. 1 fits the empirical relation of Eq. (1) with $\alpha=1.90$ and $\mu_0=1.95 \times 10^4 \text{ cm}^2 \text{ V}^{-1} \text{ s}^{-1}$. The peak mobilities are, as in Gold's theory, predicted to depend on N_{ox} as

$$\begin{aligned} \mu_p(001) &= (1.69 \times 10^3 \text{ cm}^2 \text{ V}^{-1} \text{ s}^{-1}) \\ &\times (N_{ox}/10^{12} \text{ cm}^{-2})^{-0.80}, \\ n_p(001) &= (3.63 \times 10^{12} \text{ cm}^{-2}) (N_{ox}/10^{12} \text{ cm}^{-2})^{0.42}. \end{aligned} \quad (2a)$$

$$(2b)$$

The exponents are essentially those reported in Ref. 2 (-0.79 and 0.43 , respectively), but the simple theory overestimates μ_p and underestimates n_p (Ref. 2 gives $\mu_p=1.25 \times 10^3 \text{ cm}^2 \text{ V}^{-1} \text{ s}^{-1}$ and $n_p=4.8 \times 10^{12} \text{ cm}^{-2}$ for $N_{ox}=10^{12} \text{ cm}^{-2}$), by not taking localization into account. According to our calculation, when n_d is kept fixed at $3.6 \times 10^{11} \text{ cm}^{-2}$, $\mu_p(001)$ varies approximately as $\Lambda^{-2} \Delta^{-2}$ while α depends basically on Λ , with a slight increase as Δ increases. We have also established, within the simple model, that N_d (and thus substrate doping for no applied substrate bias) is quite determinant of the theoretical results: the empirical relation of Eq. (1) is predicted only for depletion charge densities of a few times 10^{11} cm^{-2} . The exponents α , as well as μ_0 , are decreasing functions of N_d . However, as N_d approaches either 10^{11} or 10^{12} cm^{-2} , deviations from the straight-line behavior are predicted, as shown in Fig. 2.

The conclusion can be drawn that, from a theoretical viewpoint, the basic reason for the behavior noted by

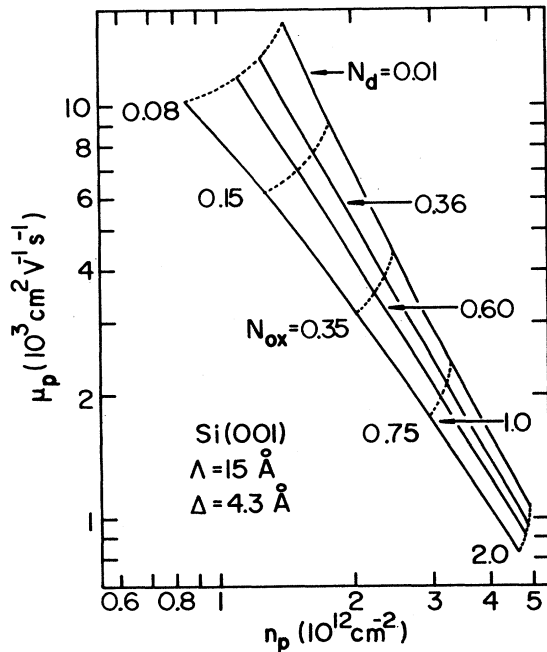


FIG. 2. Dependence on depletion charge density N_d of presently calculated $\mu_p(n_p)$ for Si(001). Equation (1) is satisfied only for N_d in the neighborhood of $0.4 \times 10^{12} \text{ cm}^{-2}$. Both N_d and N_{ox} are expressed in units of 10^{12} cm^{-2} .

Cham and Stern is the similarity of the parameters Λ and Δ which characterize the samples of different origins.

We have investigated the 4.2-K electron peak mobilities in Si(*l*ln) inversion layers, obtained by rotating from the (001) plane by an angle θ around $[1\bar{1}0]$. We have used a set of samples spanning the range $0^\circ \leq \theta \leq 43^\circ$, namely (001), $\theta=0^\circ$; (118), $\theta=10^\circ$; (114), $\theta=19.5^\circ$; (113), $\theta=25.2^\circ$; (112), $\theta=35.2^\circ$; (223), $\theta=43.3^\circ$. For each direction there were samples which allowed either for conductance measurement parallel or perpendicular to the rotation axis $[1\bar{1}0]$. The samples were made by the Toshiba Co., and are described in a paper by Sato *et al.*,⁵ who investigated anisotropic transport at $T \geq 77 \text{ K}$.

Our experimental results for peak mobilities are shown in Fig. 3 and compared to the behavior observed for Si(001). Present results for current along $[1\bar{1}0]$ do not fall very far out the limits of dispersion for Si(001), although $\mu_p(\theta > 0^\circ)$ tend to get lower as θ increases. On the other hand, μ_p 's for current perpendicular to $[1\bar{1}0]$ clearly deviate more from the general Si(001) trend, the higher the tilt angle, with both μ_p and n_p becoming lower than those corresponding to current parallel to the rotation axis. Although a small number of samples were available, the fact that the points (μ_p, n_p) tend to form clusters or lines well resolved in θ , and whose position moves monotonically out from the (001) band in Fig. 3 as θ increases, is a clear indication that the tilted samples must be modeled by a mobility calculation that takes into account at least their intrinsic Fermi-surface anisotropy.

Based on the conclusions stated previously, we restrict ourselves to linear-scattering theory. The Boltzmann equation for the out-of-equilibrium distribution function $f_1(\mathbf{k})$ is

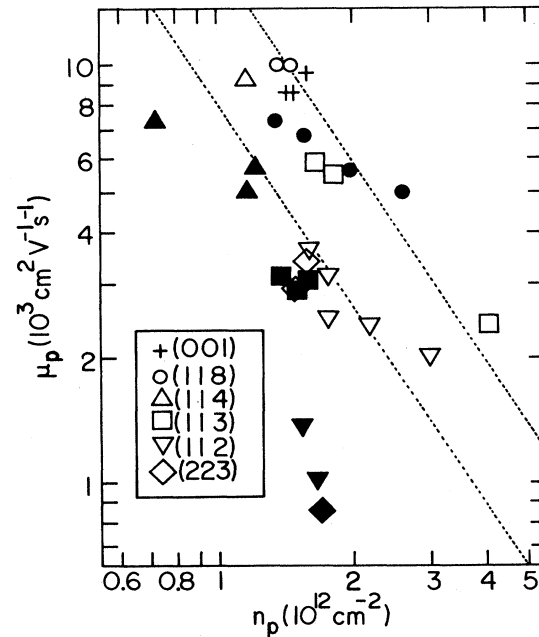


FIG. 3. Present experimental results for Si(*l*ln) inversion layers at 4.2 K. The open symbols refer to channel current in the $[1\bar{1}0]$ direction, the solid ones to current perpendicular to $[1\bar{1}0]$. Dotted lines are the dispersion limits of experimental data collected in Ref. 1 for Si(001).

$$\begin{aligned}
& e \mathbf{E} \cdot \mathbf{v}(\mathbf{k}) [\partial f_0(\varepsilon(\mathbf{k})) / \partial \varepsilon(\mathbf{k})] \\
& = (2\pi / \hbar) \sum_{\mathbf{k}'} V_{\text{sc}}^2(\mathbf{k} - \mathbf{k}') [f_1(\mathbf{k}) - f_1(\mathbf{k}')] \\
& \quad \times \delta(\varepsilon(\mathbf{k}) - \varepsilon(\mathbf{k}')) , \quad (3)
\end{aligned}$$

where $V_{\text{sc}}^2(\mathbf{q})$ is the averaged squared matrix element of the screened scattering potential, given by the sum of a contribution from ionized impurities in the Si-SiO₂ interface, $V_{\text{ox,sc}}^2(\mathbf{q})$, proportional to N_{ox} , and another contribution from the interface roughness, $V_{\text{sr,sc}}^2(\mathbf{q})$, proportional to $\Delta^2 \Lambda^2 \exp(-\Delta^2 q^2)$. The complete expressions used for $V_{\text{ox,sc}}^2(\mathbf{q})$ and $V_{\text{sr,sc}}^2(\mathbf{q})$ can be found, for instance, in Ref. 4.

For the surfaces studied, denoting the two-dimensional wave-vector components parallel and perpendicular to $[1\bar{1}0]$ by \mathbf{k}_{\parallel} and \mathbf{k}_{\perp} , respectively, the constant-energy surfaces in the independent-valley approximation are given by

$$eE \hbar m_{\parallel}^{-1} \alpha^{1/2} g \cos \phi [\partial f_0(\varepsilon_g) / \partial \varepsilon_g] = (2\pi / \hbar) N_1 (2\pi)^{-1} \int_0^{2\pi} d\phi' V_{\text{sc}}^2[\mathbf{q}(g, g', \phi, \phi')] [f_1(g, \phi) - f_1(g, \phi')] , \quad (8)$$

where $N_1 = m_d / 2\pi \hbar^2$ is the single-valley density of states per spin direction. Writing

$$W(g, \phi, \phi') = (2\pi / \hbar) N_1 V_{\text{sc}}^2[\mathbf{q}(g, g', \phi, \phi')] \quad (9)$$

and

$$f_1(g, \phi) = eE \hbar m_{\parallel}^{-1} \alpha^{1/2} g [\partial f_0(\varepsilon_g) / \partial \varepsilon_g] F(g, \phi) , \quad (10)$$

we obtain

$$\cos \phi = (2\pi)^{-1} \int_0^{2\pi} d\phi' W(g, \phi, \phi') [F(g, \phi) - F(g, \phi')] . \quad (11)$$

The solution to Eq. (11) can be obtained as a Fourier expansion,

$$F(g, \phi) = \sum_{n=1}^{\infty} F_n(g) \cos(n\phi) , \quad (12)$$

giving

$$\delta_{m,1} = \sum_{n=1}^{\infty} W_{mn}(g) F_n(g) , \quad m = 1, 2, 3, \dots \quad (13)$$

with

$$\begin{aligned}
W_{mn}(g) &= (2\pi^2)^{-1} \int_0^{2\pi} d\phi \int_0^{2\pi} d\phi' W(g, \phi, \phi') \cos(m\phi) \\
& \quad \times [\cos(n\phi) = \cos(n\phi')] . \quad (14)
\end{aligned}$$

The current in the parallel direction, taking into account a factor of 4 for spin and valley degeneracy, is

$$\begin{aligned}
j_{\parallel} &= -4e \sum_{\mathbf{k}} f_1(\mathbf{k}) V_{\parallel}(\mathbf{k}) \\
&= 4e \sum_g f_1(g, \phi) \alpha^{1/2} (\hbar g / m_{\parallel}) \cos \phi \quad (15)
\end{aligned}$$

and, substituting Eq. (10) into Eq. (15), we finally get

$$\varepsilon = \varepsilon(\mathbf{k}) = \hbar^2 k_{\parallel}^2 / 2m_{\parallel} + \hbar^2 k_{\perp}^2 / 2m_{\perp} , \quad (4)$$

and the velocities by

$$\mathbf{v}(\mathbf{k}) = \hbar^{-1} d\varepsilon(\mathbf{k}) / d\mathbf{k} = \hbar \mathbf{k}_{\parallel} / m_{\parallel} + \hbar \mathbf{k}_{\perp} / m_{\perp} . \quad (5)$$

Using the transformation

$$k_{\parallel}^2 = (m_{\parallel} / m_{\perp})^{1/2} g_x^2 = \alpha g_x^2 = \alpha g^2 \cos^2 \phi , \quad (6a)$$

$$k_{\perp}^2 = (m_{\perp} / m_{\parallel})^{1/2} g_y^2 = \alpha^{-1} g_y^2 = \alpha^{-1} g^2 \sin^2 \phi , \quad (6b)$$

$$\mathbf{q} = \mathbf{k} - \mathbf{k}' = \mathbf{q}(g, g', \phi, \phi') , \quad (6c)$$

the constant-energy surface are mapped into circles

$$\varepsilon = \varepsilon_g = \hbar^2 g^2 / 2m_d , \quad m_d = (m_{\parallel} m_{\perp})^{1/2} . \quad (7)$$

Choosing the field along the parallel direction, Eq. (3) becomes

$$\begin{aligned}
\sigma_{\parallel} &= j_{\parallel} E^{-1} \\
&= (e^2 4 N_1 / m_{\parallel}) \int_0^{\infty} d\varepsilon_g [-\partial f_0(\varepsilon_g) / \partial \varepsilon_g] \varepsilon_g F_1(g) \quad (16)
\end{aligned}$$

and

$$\sigma_{\parallel}(T=0) = n_s e \mu_{\parallel}(T=0) , \quad \mu_{\parallel}(T=0) = e F_1(g_F) / m_{\parallel} . \quad (17)$$

Successive approximations for $F_1(g)$ can be obtained by truncating the system of Eq. (13) to an increasing number of M equations, $M = 1, 2, 3, \dots$. We have found, by direct numerical computation up to $M = 3$, for all surfaces, that the lowest-order ($M = 1$) approximation gives results accurate to 5%. We have therefore used the approximation

$$\mu_{\parallel}(T=0) = e \tau_{\parallel}(g_F) / m_{\parallel} \quad (18)$$

with

$$\begin{aligned}
\tau_{\parallel}^{-1}(g_F) &= W_{11}(g_F) \\
&= (2\pi^2)^{-1} \int_0^{2\pi} d\phi \int_0^{2\pi} d\phi' W(g_F, \phi, \phi') \\
& \quad \times \cos \phi (\cos \phi - \cos \phi') \quad (19)
\end{aligned}$$

and

$$\mu_{\perp}(T=0) = e \tau_{\perp}(g_F) / m_{\perp} \quad (20)$$

with $\tau_{\perp}(g_F)$ obtained by substitution of $\cos \phi, \cos \phi'$ by $\sin \phi, \sin \phi'$ in Eq. (19).

Based on this approximation, we have extracted the peak mobility and densities for both directions, for each surface. The theoretical predictions are displayed in Fig. 4 for several values of N_{ox} , Δ , and Λ .

The first noticeable fact is that, keeping the material parameters N_{ox} , Λ , Δ , and N_d fixed, the mobilities in the perpendicular direction decrease with an increase in θ , while in the parallel direction they increase with θ . Qualitatively, this is caused by the strong screening in inver-

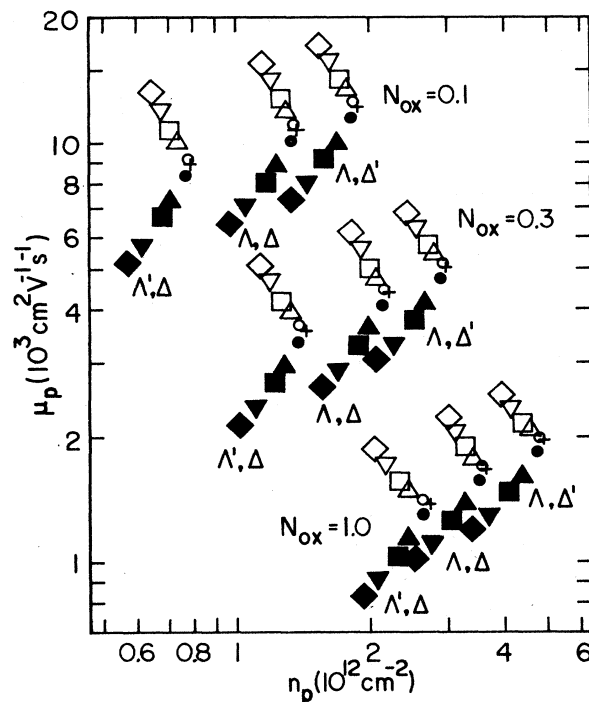


FIG. 4. Calculated peak mobilities for some $(11n)$ silicon surfaces tilted from (001) by $0^\circ \leq \theta \leq 43.3^\circ$. The symbols are the same used in Fig. 3, and Λ , Λ' , Δ , and Δ' have the same values as in Fig. 1. Values for N_{ox} are in units of 10^{12} cm^{-2} .

sion layers: $\tau \sim (\text{Thomas-Fermi wave vector})^2 \times (\text{density of states})^{-1} \sim m_d^2 m_d^{-1} \sim m_d$, and thus $\mu_{\parallel}/\mu_{001} \sim m_d/m_{\parallel} > 1$, and $\mu_{\perp}/\mu_{001} \sim m_d/m_{\perp} < 1$. Of course, only the full calculation gives the n_s dependence of these ratios.

The dependence on the material parameters of the relations between μ_p , n_p , and N_{ox} remains the same for all surfaces studied, within the accuracy of the approximation: the exponents in Eqs. (2a) and (2b) relating μ_0 and n_p to n_{ox} are approximately the same and, for fixed N_d and N_{ox} , μ_p varies approximately linearly with $\Delta^{-2} \Lambda^{-2}$, with α depending basically on Λ , reflecting the dependence of the surface roughness-limited mobility on these parameters.

Thus, by the qualitative comparison of the experimental data of Fig. 3 with the theoretical results in Fig. 4, we conclude the following.

(i) The density of Coulomb scatterers in the SiO_2 , near or at the interface, increases with tilt θ from (001) in real

samples: the peak mobilities displayed in Fig. 3 show a clear trend to monotonically decrease with tilt angle, while calculation for a fixed N_{ox} actually predicts the opposite behavior for current along the rotation axis $[1\bar{1}0]$ and just a slight decrease of μ_p with θ for current perpendicular to $[1\bar{1}0]$: it is well known,⁶ for instance, that under same oxidation conditions the density of fixed charges in the oxide depend on substrate orientation, increasing from Si(001) to Si(111).

(ii) Experimental data for n_p decrease faster with θ than expected from theory, mainly for current direction perpendicular to $[1\bar{1}0]$, that is, slightly higher Λ , Δ , or both, would also have to be associated to higher tilt angles in order to fit the results; microscopic inspection on Si-SiO₂ interfaces⁷ tend to support this result.

A straightforward way to confirm and quantify trends (i) and (ii) above is to study tilted samples in which the effective N_{ox} is controlled by driving the ionic sodium closer to or farther from the interface.⁸ Different inclinations α on log-log plots of $\mu_p(n_p)$ for samples in different directions θ would measure the variation of Λ and θ , while a changing μ_0 would measure the variation of Δ .

Another possibility is to look for such systematic interplanar anisotropies through full n_s range fittings of $\mu(n_s)$. The linear-scattering theory does not, however, provide a satisfactory fit, as it does not account for localization effects at low n_s , nor for minigap effects⁹ in tilted surfaces. For (118), for example, minigap structures in the mobility occur close to peak mobility concentration, being responsible for the slight deviation, observed in Fig. 3, from the monotonic decrease of μ_p with θ . For surfaces of higher tilt, however, these anomalies do not hinder an overall $\mu(n_s)$ fitting, because the structures are quite smooth and centered near or beyond the limit of attainable concentration.¹⁰ Preliminary fittings through linear-scattering theory for the high range of concentration have pointed to a systematic behavior of Λ and Δ with tilt: the adjusted values of Λ increased monotonically from about 10 Å for Si(001) to 25–30 Å for Si(223), while Δ changed from 3–4 Å for Si(001) to 5 Å for Si(223). The confirmation of these trends requires the extension of multiple-scattering theory to anisotropic systems. Such calculations are in progress.

The samples were kindly provided by Y. Takeishi and H. Maeda, and we would like to acknowledge useful discussions with P. J. Stiles.

¹K. Chan and F. Stern, Bull. Am. Phys. Soc. **26**, 316 (1981).

²A. Gold, Phys. Rev. Lett. **54**, 1079 (1985).

³Y. Matsumoto and Y. Uemura, in *Proceedings of the Second International Conference on Solid Surfaces, Kyoto, Japan, 1974* [Jpn. J. Appl. Phys. Suppl. **2**, Pt. 2, 367 (1974)].

⁴T. Ando, J. Phys. Soc. Jpn. **43**, 1616 (1977).

⁵T. Sato, Y. Takeishi, H. Hara, and Y. Okamoto, Phys. Rev. B **4**, 1950 (1971).

⁶P. Balk, P. J. Burkhardt, and L. V. Gregor, IEEE Proc. (Corresp.) **53**, 2133 (1965).

⁷S. M. Goodnick, R. G. Gann, J. R. Sites, D. K. Ferry, C. W.

Wilmsen, D. Fathy, and O. L. Krivanek, J. Vac. Sci. Technol. B **1**, 803 (1983).

⁸A review of the results on minigaps in tilted silicon surfaces up to 1979 is given by V. A. Vokov, V. A. Petrov, and V. B. Sandomirskii, Usp. Fiz. Nauk **131**, 423 (1980) [Sov. Phys.—Usp. **23**, 375 (1980)].

⁹A. Hartstein, A. B. Fowler, and A. Albert, Surf. Sci. **98**, 181 (1980).

¹⁰J. B. Veiga Salles, H. Closs, J. R. Senna, and P. J. Stiles, Phys. Rev. B **37**, 3912 (1988).